Author's Accepted Manuscript

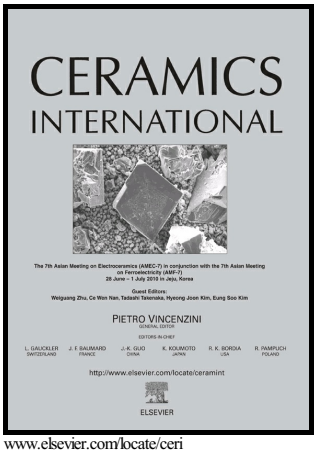

www.elsevier.com/locate/ceri

The properties of hydroxyapatite ceramic coatings produced by plasma electrolytic oxidation

S.A. Adeleke, S. Ramesh, A.R. Bushroa, Y.C. Ching, I. Sopyan, M.A. Maleque, S. Krishnasamy, Hari Chandran, H. Misran, U. Sutharsini

PII: S0272-8842(17)32306-4
DOI: https://doi.org/10.1016/j.ceramint.2017.10.114
Reference: CERI16533

To appear in: *Ceramics International*

Received date: 7 October 2017
Revised date: 17 October 2017
Accepted date: 17 October 2017

Cite this article as: S.A. Adeleke, S. Ramesh, A.R. Bushroa, Y.C. Ching, I. Sopyan, M.A. Maleque, S. Krishnasamy, Hari Chandran, H. Misran and U. Sutharsini, The properties of hydroxyapatite ceramic coatings produced by plasma electrolytic oxidation, *Ceramics International,* https://doi.org/10.1016/j.ceramint.2017.10.114

This is a PDF file of an unedited manuscript that has been accepted for publication. As a service to our customers we are providing this early version of the manuscript. The manuscript will undergo copyediting, typesetting, and review of the resulting galley proof before it is published in its final citable form. Please note that during the production process errors may be discovered which could affect the content, and all legal disclaimers that apply to the journal pertain.

ACCEPTED MANUSCRIPT

The properties of hydroxyapatite ceramic coatings produced by plasma electrolytic oxidation

S.A. Adeleke[1], S. Ramesh[1,*], A.R. Bushroa[1], Y.C. Ching[1], I. Sopyan[2], M.A. Maleque[2], S. Krishnasamy[3], Hari Chandran[4], H. Misran[5], U. Sutharsini[6]

[1]Center of Advanced Manufacturing and Material Processing, Department of Mechanical Engineering, Faculty of Engineering, University of Malaya, 50603 Kuala Lumpur, Malaysia

[2]Department of Manufacturing and Materials Engineering, International Islamic University Malaysia, P.O. Box 10, 50728, Kuala Lumpur, Malaysia

[3]Department of Surgery, Faculty of Medicine, University of Malaya, 50603 Kuala Lumpur, Malaysia

[4]Division of Neurosurgery, Faculty of Medicine, University of Malaya, 50603 Kuala Lumpur, Malaysia

[5]Nanoarchitectonic Laboratory, Department of Mechanical Engineering, College of Engineering, Universiti Tenaga Nasional, 43000 Kajang, Selangor, Malaysia

[6]Department of Physics, University of Jaffna, Jaffna, JA 40000, Sri Lanka

[*]Corresponding author.: ramesh79@um.edu.my

Accepted manuscript

Abstract

Calcium phosphate coatings produced on the surface of Ti6Al4V by plasma electrolytic oxidation (PEO) using different concentrations of hydroxyapatite (HA) in a 0.12 M Na_3PO_4 (NAP) electrolyte solution was investigated. It was found that the amount of calcium phosphate particles infiltrated into the coating layer as well as the thickness and the surface

ACCEPTED MANUSCRIPT

roughness of the coating increased with increasing HA concentration. The porosity of the ceramic coatings indicated an inverse relationship with the concentration of HA particles dispersed in the NAP solution. The result also demonstrates that higher scratch adhesive strength was achieved using 1.5 g/L HA solution, producing a critical load of 2099 mN, while 0 g/L HA only produced a critical load of 1247 mN. The adhesion becomes independent of thickness when the concentration of HA exceeds 1.5 g/L. The failure of the coating was characterized by large periodic hemispherical chipping, while intermittent delamination was noticed with the coating embedded with HA particles. This study demonstrate the viability of using PEO to produce a thin layer of HA ceramic coating on Ti6Al4V suitable for biomedical applications.

Keywords

Plasma electrolytic oxidation; hydroxyapatite coating; coating characteristics

1. Introduction

Titanium (Ti) and its alloys have been the material of choice for orthopaedic and dental implants because of its excellent properties, including high strength to weight ratio, corrosion resistance, bioinert and the passive oxide layer formation on the surface of Ti possesses superior chemical stability. However, this native oxide film, which is of the order of a few nanometres, exhibits poor biological bonding with the surrounding tissues [1]. Titanium-based materials do not form a good chemical bond to the bone tissues because of its non-bioactive characteristics [2]. Owing to this, enhancement of its bioactivity has been the key research focus.

One of the viable means to improve the bioactive properties of Ti is by altering its surface chemistry through the incorporation of a calcium phosphate (CaP) on the implant

Accepted manuscript

ACCEPTED MANUSCRIPT

surface [3]. The deposition of CaP on Ti surface facilitates the direct bone formation and differentiation of bone forming cells on the implant surface. For the past few decades, several coating techniques have been experimented to deposit CaP on the surface of metallic implants including sol-gel [4], plasma spray [5], and electrophoretic deposition [6]. However, there are several drawbacks associated with these techniques which include poor adhesion of the coating on the substrates, non-uniform coating formation over geometric complex surfaces, and low crystallinity as reported by Tahmasbi Rad et al. [7], from their research work of bio-physical performance of HA coating using electrophoretic deposition method. Hence, there has been an increasing demand in recent years to develop other viable coating technique [8].

Plasma electrolytic oxidation (PEO), also known as micro-arc oxidation has been gaining popularity as a unique surface engineering technique to produce a highly adherent bioactive and micro-porous layer on implant surfaces [9]. PEO is a relatively new electrochemical surface treatment using a hybrid of conventional electrolysis and plasma arc discharge within an electrolyte solution under high voltage. It is an advanced surface engineering coating technique for producing ceramic coating on light materials such as Ti, Al, Mg, Zr and their alloys. Among the other advantages of PEO are its simplicity, low cost, ability to form complex compounds using eco-friendly solutions and ability to form uniform coatings on complex geometries as pointed out by Sandhyarani et al. [10] while investigating the effect of treatment time on ZrO_2/HA fabrication on zirconium substrate by PEO method.

In a typical PEO process, the working electrode (anode), together with the counter electrode (cathode), usually stainless steel of a larger surface area is immersed into a suitable electrolyte of interest. An external power supply is connected to the two electrodes providing the energy necessary for the coating process. At a sufficiently high potential difference of a few hundred volts, the electrolyte compound dissociates into anions and cations. The anions

Accepted manuscript

ACCEPTED MANUSCRIPT

drift towards the working electrode (e.g. Ti, Al, Zr and Mg) while the cations migrate towards the cathode. At the anode, the oxidation of the surface starts by forming an insulating layer on the working electrode which causes a slight drop in the applied current. With a further increase in the applied voltage, the intense electric field between the electrodes generates a micro-arc plasma discharge on the anodic surface, transforming it to a micro-porous thin oxide layer. The deposition of electrolyte ingredients then follows. The coating is formed on the entire substrate (anode) immersed in the electrolyte solution without altering the bulk properties of the substrate material. In addition, the composition of the oxide film can be controlled by adjusting the components in the electrolyte and the concentration of the electrolyte [11]. Some researchers have focused on improving the bioactivity of the Ti alloy surface by incorporating Ca and P ions in the surface oxide layer. For instance, Faghihi-Sani et al. [12] demonstrated that chemical treatments of the micro-arc oxidized layer via immersion in NaOH solution enhanced the apatite formation ability of Ti alloy. The increase in crystallinity of HA was attributed to higher concentration of OH^- on the oxide layer containing Ca^{2+} and PO_4^{3-} ions. Sowa et al. [13] investigated the bioactivity of anodic oxide coating on Ti13Nb13Zr by PEO process in a solution containing Ca and P. They observed that the thick oxide surfaces were essentially amorphous, with small amount of crystalline phases, depending on the PEO process parameters. The obtained oxide coatings were reported to improve after 4 weeks of immersion in SBF. The results showed that PEO can allow the diffusion of Ca and P ions into the surface of the porous oxide in the form of an amorphous phase, and further hydrothermal treatment can successfully transform the amorphous phase into crystalline HA.

Teng et al. [14] studied the feasibility of obtaining HA by pre-immersion of micro-porous TiO_2 layer in a weak base electrolyte, KH_2PO_4. The growing of Ti-OH bonds on the surface of the oxide layer assisted the growth of HA when immersed in simulated body fluid

Accepted manuscript

ACCEPTED MANUSCRIPT

(SBF). Few successful results of HA formation on the surface of PEO layers, either by hydrothermal treatment or immersion in SBF, have been reported. Studies have shown that the bioactivity of Ti surface can be increased with incorporation of Ca and P ions in the oxide film. However, there are few literature reports on how the level of these elements affects the PEO-derived oxide film layer. Moreover, the mechanical integrity of the oxide film before and after incorporation with Ca and P ions has not been systematically investigated.

In this study, a single process of PEO was used to produce films incorporating HA, and the effect of various HA concentrations in the oxide film on the Ti6Al4V alloy substrate were examined. Comparisons were made of the concentration of HA associated with the porous oxide film, allowing an understanding of how Ca and P ions are incorporated during formation of porous layer. Sodium phosphate (Na_3PO_4), an inexpensive, benign and familiar compound, was chosen as the electrolyte. This selection is based on the fact that PO_4^{3-} from Na_3PO_4 has the ability to negatively charge the HA particles during the PEO process. This is the first report of the use of Na_3PO_4 as the solitary electrolyte for HA particle deposition. The effect of the HA particle concentration in the Na_3PO_4 electrolyte solution on the surface structure, thickness, roughness, porosity and elemental composition of the coating layer were investigated. The adhesion behaviour of coatings produced with different HA concentrations was also studied, and the mode of failure of coatings with and without HA particles was analysed.

Accepted manuscript

2. Materials and methods

2.1. Substrate Preparation

Ti6Al4V (Grade 5) plates (Cenco Sains Special Materials Co. Ltd, Malaysia) were used as the substrates in this study. The Ti substrates ($20 \times 10 \times 2$ mm^3) were prepared and abraded using SiC emery paper up to 2000 grade. The abraded surface was cleaned with

ACCEPTED MANUSCRIPT

acetone and distilled water in an ultrasonic bath, and finally dried in air. Two stages of cleaning were used to ensure that the surface is clean and free from contaminants before the plasma electrolytic treatment.

2.2. Preparation of the electrolyte containing HA particles

HA aqueous suspensions were prepared by adding commercially available HA powder (Sigma-Aldrich) to 0.12 M sodium phosphate solution. The concentrations of HA particles in the four suspensions were 0, 1, 1.5 and 2 g/L, respectively. Prior to the PEO process, the aqueous HA suspension was stirred using a magnetic stirrer for 1 h and then sonicated using an ultrasonic bath cleaner for 2 h to prevent settling and agglomeration of the HA particles.

2.3. Fabrication of PEO-coatings on the substrate surface

For plasma electrolytic oxidation process, the electrolyte prepared was placed into a stainless steel container which serves as the counter electrode (cathode), and the working electrode (Ti6Al4V substrate) was immersed in the electrolyte to serve as the anode. The PEO treatment was carried out at a constant current density of 0.5 Adm^{-2}, a voltage of 300 V and a deposition time of 5 min using an auto-ranging DC power supply unit (Keysight Technologies Deutschland GmbH, Model No: N8957A, Germany) with a maximum voltage of 1500 V and current of 30 A capacity. After the PEO process, the coated samples were rinsed with distilled water, air dried and kept in a desiccator prior to characterization. The electrolyte temperature did not exceed 35 °C during the PEO. The PEO coating parameters used in the experiment are summarized in Table 1. The identification code for the PEO

Accepted manuscript

ACCEPTED MANUSCRIPT

treated substrates using the electrolytes with HA particle concentrations of 0, 1, 1.5 and 2 g/L hereafter represented as S_0, S_1, $S_{1.5}$ and S_2, respectively, while the untreated substrate was referred to as 'Ti'.

2.4. Surface characterization of TiO_2/HA coated samples

The surface morphology and elemental composition of the samples were analysed using a high-resolution field emission scanning electron microscope (FESEM) and an energy dispersive spectrometer (EDS) (FESEM-EDS, FEI Quanta 450 FEG). The phase composition of the samples was studied by X-ray diffraction (XRD; PANalytical X'Pert High Score Empyrean, 45 kV, 40 mA) with a CuK_α (λ=1. 54) radiation over the scanning range (2θ) from 10^o to 80^o with a scan speed of 1° min^{-1} and a step size of 0.02°. The roughness of (R_a) of untreated substrate (Ti) and coated samples was measured using a Mitutoyo Surftest SJ-201 profilometer. For every measurement, five samples were tested and average value taken. The images of the microstructures taken by the FESEM were analysed using OLYMPUS Stream Micro-Imaging Software to measure the percentage porosity of the coated samples.

2.5. Micro-scratch test

A micro-scratch tester (Micro Materials Ltd., Wrexham, UK) was used to measure the adhesive strength of the TiO_2/HA coating by applying a load ranging from 0 to 2500 N, which generated scratches with a conical Rockwell diamond tip of radius 25 μm. The indenter was drawn across the coated surface to be tested under progressive loading at a fixed rate of 1.2 μm/s. The scratch length during the scratch test was 1000 μm. In the micro-scratch test, critical load (L_c) was used to quantify the adhesive strength of coating/substrate combinations and it was defined as the load that caused the coatings to detach completely

Accepted manuscript

ACCEPTED MANUSCRIPT

from the substrate. The critical load value was confirmed by the scratch tracks. The chronology of the abrupt changes along the profile determined the critical loads on the scratch track, which were defined as (a) $L_{e\text{-}p}$: critical load for the onset of plasticity; (b) Lc_1: critical load to indicate onset of edge cracking; Lc_2: critical load to indicate delamination of film from the substrate; Lc_3: critical load of total coating failure as indicated by complete exposure of the substrate surface. To determine the magnitude of the critical load, the frictional curve and penetration depth as a function of critical load were also measured. After the scratch test, the scratch tracks were observed using the FESEM and optical microscope to evaluate the damage and changes in morphology on the as-deposited coatings.

3. Results and discussions

3.1. Voltage-time response of PEO coatings

Monitoring the voltage-time response is important to understand the electrochemical behaviour of the samples during the PEO process. The voltage-time plots obtained during the PEO processing of Ti alloy under various electrolyte concentrations are shown in Fig. 1. During the first 30-50 s, the voltage rises fast and increases linearly with time at a constant rate. This initial rise in voltage is due to dissolution of the substrate and formation of a thin oxide layer at the electrolyte/anode interface.

For the sample S_0, the dissolution-oxide film formation is observed up to approximately 199 V, where dielectric breakdown of the film (normal oxide growth terminates) and numerous micro-arc sparks along with fine discharges were noticed on the sample surface. This was also accompanied by gas evolution. This behaviour continues until a final voltage of 300 V was registered. At this point, no significant increase in the intensity of the micro-sparks was observed on the substrate. The emergence of high frequency

Accepted manuscript

ACCEPTED MANUSCRIPT

ascending and descending oscillation of the cell voltage, observed for the S_1, $S_{1.5}$ and S_2 samples, represents the stages of oxide breakdown and regrowth, which maintains the thickness of the layer approximately constant. The distinct deviation in the observed behaviour of the S_1, $S_{1.5}$ and S_2 samples, compared to S_0, is due to the electrolyte concentrations at the oxide interface. During the PEO process, when a current density flows through the anode/electrolyte interface, the charged electrolyte particles (HA) enter the initial growing oxide layer and release a current of electrons into the oxide film. The incorporation of ions into the oxide film induces a complex high-temperature reaction and causes the initial growth layer to lose its oxide coating (initial breakdown). This enables an avalanche of electrons injections into the broken spot, thus allowing the locally destroyed film to be rebuilt immediately. As soon as the breakdown is eradicated, the anodization proceeds further to a new breakdown voltage, when the ionic current in the oxide film predominates. This phenomenon continues until a final voltage is reached. It has been shown in Albella and Martinez-Duart [15] and Ding et al. [16] work, that the working voltage and the final voltage during the PEO process decrease with increasing electrolyte concentration due to the electrolytic composition, and therefore it is not surprising that the highest electrolyte concentration, S_2, exhibited the lowest final voltage. While the increase in voltage during the PEO process up to the point of breakdown voltage is predominantly governed by the electrolyte concentration, the further increase in voltage is caused by the growth of the layer thickness and coating formation on the substrate surface. The final voltages reached at the end of coating of S_0, S_1, $S_{1.5}$ and S_2 in the present study were 300, 296, 278 and 252 V, respectively.

3.2. Morphological and elemental analysis of the PEO coating

Accepted manuscript

ACCEPTED MANUSCRIPT

The surface morphology of the polished substrate surface and of the coatings produced by PEO at different HA concentrations are shown in Fig. 2. It is obvious that the surface morphology was affected by the HA concentration in the NAP electrolyte solutions. Without HA, the coating surface is covered by many discharge channels appearing as irregular circular and elliptical spots distributed over the entire film surface (Fig. 2b). The spots seem to be associated with the liberation of gaseous oxygen and micro-arc discharge occurring on the Ti surface. When the Ti surface was treated with a solitary NAP electrolyte solution, a careful observation of micro-arc discharge revealed that oxidation of the surface started to occur at ~ 164 V and became more intense with increasing electrolytic voltage (up to 300 V). Consequently, the micro-porous rough region started to appear locally due to the formation of an insulating TiO_2 layer on the Ti surface. The Ti surface which was initially smooth (Fig. 2a) became rough with numerous micro-pores due to the high spark discharges and gas evolution.

For sample processed with a lower HA concentration (S_1), the film surface was seen to be rough and a number of micro-pores were observed. However, the micro-pores are not as prominent as those observed without HA addition. The large micro-pores noticed without HA addition became slightly smaller. This indicates that the pores have partially been sealed by the HA particles. Nevertheless, the surface appeared to maintain the initial surface morphology of the PEO-NAP treated layer. A tiny surface crack was found on the surface processed with S_1 concentration. The residual stress developed during the PEO process due to rapid solidification seems to be the main cause of cracking. With a further increase of the HA concentration (from 1.5 g/L to 2 g/L), micro-pores were hardly seen on the surface as they have been covered with HA particles.

Accepted manuscript

ACCEPTED MANUSCRIPT

In addition, at higher HA concentrations, the electrolyte fluidity increased, and the gas evolution, which usually accompanied the PEO process, was suppressed. On the other hand, the evolution of gas from the less viscous solution used for the S_1 sample during the solidification process led to the formation of pores and the electrolyte was not sufficiently fluid to fill the pores. The surface chemical composition of the PEO coatings examined by EDS is shown in Figs. 2(b-e). The coating is mainly composed of Na, Al, P, Ti and O (Fig. 2b). This means that substrate and modifying elements from the electrolyte participated in the formation of the coatings. The higher content of Ti and O from the elemental composition indicates that oxidation of the substrate is predominant during the PEO process. With the samples produced in the HA-containing NAP electrolyte solutions, the EDS spectrum showed the presence of Ca and P peaks (Figs. 2 (b-e)). This suggested that HA could be deposited in the film layers by PEO treatment in an aqueous NAP electrolyte solution. The increase in Ca and P concentration in the S_1, $S_{1.5}$ and S_2 samples confirm that HA has been incorporated into the PEO-TiO_2 coatings. The changes in the amount of Ca and P can be attributed to the different amount of HA particles in the NAP electrolyte solution. This shows that the HA concentration plays an important role in determining the amount of Ca and P incorporated in the oxide film. The temperature and pressure inside the porous layer is high enough to cause ionization of HA particles via the following reaction:

$$Ca_{10}\ (PO_4)\ (OH)_2 \rightarrow 10\ Ca^{2+}\ 6{HPO_4}^{2-} +\ 2OH^- \qquad (1)$$

This reaction is considered to be responsible for various content of Ca and P in the oxide film layer. The relative amount of Ca and P on the surface of the PEO samples is shown in Table 2. The result shows that the Ca/P ratio was highest for S_2 and that the Ca and P were relatively more abundant in the oxide film layer when higher concentrations of HA particles

Accepted manuscript

ACCEPTED MANUSCRIPT

were used. A similar phenomenon was observed by Sowa et al. [13], during PEO process of Ti13Al13Nb alloy, in which the incorporation of Ca and P species in the oxide film proceeded to a higher extent when higher concentration of calcium phosphates was used. However, the research conducted by Yao et al. [17] shows that release of additional ions into solution from higher concentrations may lead to a decrease in the content of Ca and P in the oxide film layer. This shows how the composition and concentration of the electrolyte ingredients can affect the incorporation of Ca and P in the oxide film layer. The EDS elemental mapping of the PEO-coated sample (not shown here) revealed that Ca and P elements were distributed homogeneously throughout the coating.

The XRD patterns of the PEO coatings prepared at different HA concentrations in the 0.12 M NAP solution are shown in Fig. 3. During the PEO process, the temperature and pressure in the discharge channel could reach approximately 10000 K and 100 MPa [18], which are high enough to promote the conversion of the Ti substrate into micro-porous TiO_2. At a 0 g/L HA concentration, there were only Ti and anatase TiO_2 phase (Fig. 3a). With the addition of HA, the peak associated with HA and tricalcium phosphate (TCP) were detected along with anatase (Figs. 3(b-d)). Moreover, as the HA concentration increases from 0 to 2 g/L, the intensity of the HA and TCP peaks increase. The appearance of TCP at 5 min. deposition time has also been reported by Durdu et al. [19], while studying hydroxyapatite and calcium apatite based coatings formation on Ti6Al4V alloy surface using PEO method. Abbasi et al. [20] inferred that the decomposition of HA_p phase to TCP is as a result of anode temperature surge during PEO process. They found that the HA phase appeared at a deposition time of 3 min. and its decomposition start to occur when treated above 3 min. deposition time.

Accepted manuscript

ACCEPTED MANUSCRIPT

3.2.1. Surface roughness, micro-porosity and thickness of TiO_2/HA coating

The surface roughness (R_a) of untreated Ti and the coated S_0, S_1, $S_{1.5}$, and S_2 samples are presented in Table 3. The R_a of the PEO treated layers is significantly higher than that of untreated Ti. When the Ti was micro-arc oxidized with the electrolyte with no HA additions, the surface roughness increased steadily. The surface roughness of the $S_{1.5}$ and S_2 samples were much higher than the oxidized surface (S_0). With a further increase in the HA concentration above 1.5 g/L, only a slight increment in roughness was observed, which indicates that HA addition did not alter the roughness significantly.

The polished cross-sectional views of PEO-coated surfaces of the samples prepared with different HA concentrations are shown in Fig. 4. The average coating thickness (Table 3) revealed that the thickness of the PEO-coated layers also depends on the HA content in the electrolyte. With increasing concentration of HA particles in the electrolyte during PEO treatment, a much thicker layer, ranging from 10-17 μm, was formed. The obtained coatings were significantly thicker when higher concentrations of HA were used. This finding is in agreement with the observation reported by Bai et al. [21] and Simka et al. [22] in their PEO treatment of Ti samples. They found that the thickness of oxide film was higher when larger amount of Ca and P were deposited into the porous oxide film. A significant amount of closed pores were also observed due to CaP enrichment in the porous oxide layer.

This morphological change is attributed to the dielectric breakdown of the enriched oxide layer. It can be inferred that during the PEO process, an intense micro-arc discharge

Accepted manuscript

ACCEPTED MANUSCRIPT

appears on a local area of the substrate to form micro-pores. As the micro-pores are formed, more openings are created for the entrance of electrolyte-borne particles. The micro-porous layer becomes filled with Ca and P ions. As the TiO_2 layer enriched with Ca and P becomes thicker, the resistance of the layer increases and more energy is required to break the dielectric layer. Owing to a series of thermochemical reactions and subsequent formation of complex compounds on the substrates, the roughness and thickness increase. The roughness and thickness of the PEO-coated layers depend on the electrolyte concentration and the coatings were significantly rougher and thicker when higher concentrations of HA were used.

The porosity of the PEO coatings was examined using OLYMPUS Stream Micro-Imaging Software. The results, given in Table 3 show that the porosity decreases with increasing HA particle concentration in the oxide films. The PEO coating processed with 0 g/L HA had a large percentage of pores. These pores are characteristic features of the PEO coating and their formation is related to gases produced during the PEO process. The NAP solution (without HA addition) is less viscous, and the entrapped gases produced during the PEO process formed pores on the re-solidified Ti surface (Fig. 2d). On the other hand, the PEO processed with the electrolytes with the HA addition had high fluidity due to the concentrations of HA particles. The evolved gases can escape during the solidification or sintering process when the electrolyte solution is sufficiently fluid. It is believed that the PEO coatings with HA addition yielded high fluidity liquids which assisted these gases to escape. The porosity level of the sample code S_2 decreases due to the HA incorporated into the film layer (Fig. 2e).

3.3. Mechanisms of TiO_2/HA coating formation

The deposition of HA in the Na_3PO_4 solution was performed using an anodization process, and a TiO_2/HA layer is created on the Ti surface. In the PEO process, when the

Accepted manuscript

ACCEPTED MANUSCRIPT

applied voltage is higher than the breakdown voltage, the micro-arc discharges rapidly build up on the anode surface which leads to the dissolution of Ti metal. According to Eq. (2), Ti plate has a strong tendency to release electrons to produce Ti^{4+} ions.

$$Ti \rightarrow Ti^{4+} + 4e^{-} \quad (2)$$

At a sufficient potential difference, the water molecules in the aqueous electrolyte solution dissociate and produce hydroxyl (OH^{-}). The OH^{-} ions migrates towards the anode and produces O_2 gas via the following chemical reactions.

$$2H_2O \rightarrow H_3O^{+} + OH^{-} \quad (3)$$

$$4OH^{-} \rightarrow O_2 + 2H_2O + 4e^{-} \quad (4)$$

Thus, the main reactions occur on the anode via the combination of equations (2 and 4) as follows:

$$Ti + 4OH^{-} \rightarrow TiO_2 + 2H_2O + 4e^{-} \quad (5)$$

In the next stage of the PEO process, the Na_3PO_4 compound in the electrolyte can ionize to Na^{+} and PO_4^{3-}. The anion (PO_4^{3-}) is not bound to any particular atom during the PEO process and are free to drift throughout the entire electrolyte bath, which finally form a sea of electrons on the HA particles. The PO_4^{3-} ion charges the HA particles negatively. The negatively charged HA particles in the electrolyte are attracted to, and migrated towards, the anode under the strong electric field and get deposited into the microporous oxide layer grown via the PEO process. The HA particle is thereafter sintered onto the anodic surface by the high micro-arc plasma discharge produced at the anode. Thus, the incorporation of

Accepted manuscript

ACCEPTED MANUSCRIPT

charged HA particles into the porous oxide film will occur concurrently, thereby forming the TiO_2/HA layer.

During the PEO process, the high temperature generated inside the micro-porous layer would promote migration of Ca and P ions from the inner porous layer into the outer layer and form tricalcium phosphate according to the following reaction:

$$3Ca^{2+} + 2PO_4^{3-} \rightarrow Ca_3(PO_4)_2 \quad (6)$$

According to reaction equations (2-6), TiO_2 is produced in the anodic coatings, and Ca and P elements are incorporated into the oxide films. In addition, anatase, TCP and HA are present in the PEO coatings.

3.4. Adhesive strength of PEO coated surfaces

Adhesion of the coatings to the substrates is critical to their function and determines the stability and durability of films. Many studies have used scratch test method to examine the adhesion of coating to substrate [23]. Though Bull and Berasetegui [24] explained that several failure modes may occur during the scratch test, the actual failure mechanism is still unclear. Nevertheless, scratch test method has been demonstrated as an effective method to obtain the critical loads that are related to the adhesion properties of coatings [25]. To detect the widest possible range of coating failure modes, scratch tests were performed on PEO-coated surfaces. To assess the effect of the HA concentration of the coating, all the scratches were examined using both an FESEM and an optical microscope, and the load at which the uncovered substrate was conspicuously visible along the scratch tract was used to define the critical load.

Accepted manuscript

ACCEPTED MANUSCRIPT

Fig. 5 shows the surface of the coating after the diamond indenter is drawn over the surface with a linearly increasing load (0-2500 N) until failure occurs at the critical load (Lc_2). At the onset of the test, the coating was in the elastic-to-plastic region (*Le-p*). As the normal load progressively increases, the indentation tip gradually sinks into the coated layer, indicated by a nearly linear change of penetration at the beginning of the test (Figs. 5 (a-d)). Consequently, spalled regions of coating removed laterally from the edges of the scratch track grooves were observed. With the sample processed without the HA addition (S_0), it is observed that at a scratch length of approximately 200 μm (Fig. 5a) S_0 started to experience cohesive failure indicated by large periodic localized hemispherical chips, which remain attached to the coating at the outside edges of the trackside, indicating a weak cohesive strength of this sample. Such film failure is clearly seen as an increase in scratch depth and subsequent fluctuation of the frictional force as the indenter tip encounters broken film (Fig. 5a). This was subsequently followed by detachment of the coating and subsequent failure of the coated layer through complete exposure of the substrate material. A complete removal of the coating in the scratch track occurs at Lc_2 of 1247 mN (at a scratch length 390 μm). It is to be noted that S_0 has the lowest coating thickness and a high level of porosity (Table 3), which are thought to be responsible for the low adhesive strength. The presence of the porous thin layer led to faster degradation of the adhesive strength and early fracture under the applied load. The stylus tip could penetrate the porous thin layer more easily and thus the durability of the oxide film coating was reduced. Therefore, the failure of S_0 can be attributed to the presence of a micro-porous thin layer on the surface of this sample which weakens the interface layer. ~~It is believed that the contact area between the pore-containing oxide film and the Ti surface is reduced due to the presence and arrangement of the pores.~~

Accepted manuscript

ACCEPTED MANUSCRIPT

Comparing the samples processed without HA (S_0) with those processed with HA addition (S_1, $S_{1.5}$ and S_2), the scratch length between the chipping region and the point of delamination suggests that the coatings processed with HA addition have adequate adhesive strength. The failure mode depicts different surface features. The first sign of failure observed with the samples processed with HA addition was intermittent delamination of the coating layer along the scratch path (Figs. 5 (b-d)). This is also reflected by the intense penetration depth and fluctuation of the frictional force during the test. As the load progressively increased, the coating was seen to completely fail from the substrate surface. The extent of delamination along the scratch path is more pronounced with the highest HA addition (S_2). It is clear from the scratch test results presented here that the intermittent delamination and the area of uncovered substrate is greater and extends beyond the limit of the scratch track (Fig. 5d) for sample S_2, while the $S_{1.5}$ sample only had a small amount of exposed substrate that was confined within the track (Fig. 5c).

Adhesive strength obtained at the same scratch length revealed that the coating on S_2 begins to delaminate when it reached a scratch length of 398 μm (Lc_1) and this intermittent distortion or delamination continues until it reached a scratch length of approximately 610 μm at 1739 mN critical load (Lc_2), when it finally failed. At the same scratch length, the coating on sample $S_{1.5}$ was still intact, and only began to experience chipping film failure at a higher scratch length of 418 μm (Lc_1). The complete failure of the coating occurred at a scratch length 835 μm, corresponding to a critical load of 2099 mN (Lc_2). However, the coating on sample code S_1 failed at a scratch length of approximately 512 μm and critical load of 1514 mN.

The reason for the detrimental effect of the highest HA concentration is related to the morphological change of the TiO_2 film. The TiO_2 film enriched with the highest concentration of HA was not well formed due to the higher level of Ca and P in the anodic

Accepted manuscript

ACCEPTED MANUSCRIPT

oxide film (Fig. 2d). The incomplete breakdown of the anodic oxide/micro-arc discharges film due to high levels of Ca and P elements may have resulted in a poor network of micro-pore channel through the oxide section of the increased layer thickness (Fig. 4d). ~~Owing to this, the microstructure surface became irregular (Fig. 2e) as the Ca and P are not uniformly distributed in the oxide film~~. As a result of this, the oxide film became unstable when the HA concentration increased beyond 1.5 g/L HA. ~~This is believed to have caused a deterioration of the adhesive strength.~~

Although, S_2 has the highest coating thickness and showed the existence of strong intensity of Ca and P, its overall adhesive strength was lower than that of the sample processed with 1.5 g/L HA ($S_{1.5}$) due to instability of the oxide film and higher levels of Ca and P in the oxide film. The reduction in L_c of the thickest sample can be attributed to high levels of residual stress, which arises from the thermochemical reaction during formation of the coating. At a 2 g/L HA concentration at the anodic interface, higher incorporation of ions is expected, which will ultimately release larger exothermic energy. The gas generated during the reaction causes development of voids area and pores at the interface and centre of the cross-section of the thick layer (Fig. 4d). Thus, the adhesive strength decreases when the level of residual stresses present in the TiO_2/HA film increases. A similar result was reported when CaP was produced on Ti surface using the electrochemical deposition method. Higher thickness and surface roughness were recorded with low adhesive strength [26]. Of all the samples, $S_{1.5}$ displayed high adhesive strength and cohesive resistance to the applied stress of the sliding indenter during the scratch test.

Further investigation was done to identify the elemental constituents in the scratches produced during the scratch test. The elemental profile for the samples prepared with these two HA concentrations was also characterized by the FESEM line scan analysis as shown in Fig. 6. It can be observed from the spall region area of the scratch test (Fig. 6b) that

Accepted manuscript

ACCEPTED MANUSCRIPT

detachment of the coating in S_2 is more pronounced compared to $S_{1.5}$. For sample $S_{1.5}$, some spallation is noticed on both sides of the scratch area (Fig. 6a). Along the scratch length of the test, peaks for Ti and O were detected which indicates the existence of the oxide phase. The distribution of the oxide layer can be observed for sample code $S_{1.5}$ almost along the entire scratch length of the test. However, for sample code S_2, as the relative intensity of Ca and P ions increased, the peak of Ti decreased up to a certain limit, and this marks the beginning of the instability of the oxide film (Fig. 6b). This may be associated with the incorporation of more HA particles from the NAP electrolyte aqueous solution.

3.4.1. Scratch hardness of PEO-coated surfaces

To measure the resistance of the TiO_2/HA film to deformation, the scratch hardness test was conducted on the PEO-coated samples. This test provides a different combination of the surface as the stylus moves tangentially along the coated surface. The method is applicable to a variety of engineering materials including ceramics, metals and polymers. It involves measurements of the leftover scratch width after the stylus has been removed to calculate the hardness number. Owing to the fact that, the stress state at the diamond tip is a function of the contact area and applied force, the scratch hardness depends solely on the diamond tip radius and applied load [27]. The hardness is obtained by dividing the applied load on the diamond tip by the projected area of the contact scratching surface. In the present work, a constant normal force is applied by the stylus and track formed by relative movement of the stylus against the coated surface. The average width of the scratch track was measured with the aid of optical microscope. The scratch hardness H_{SP} was determined following the specification of ASTM G171-03 [28]:

Accepted manuscript

ACCEPTED MANUSCRIPT

$$H_{SP} = \frac{8P}{\pi w^2} \quad (7)$$

where H_{SP} is the scratch hardness number, P is the normal force (N) and w is the scratch width (mm).

The scratch hardness measured for the PEO-coated Ti processed at different HA concentrations was 5.03, 4.07, 4.96 and 3.34 GPa for the $S_{0,}$ S_1, $S_{1.5}$ and S_2 samples, respectively. The results show that the oxide film layer had the highest resistance to scratching than coatings produced with HA addition. The relatively lower hardness obtained with HA addition could be associated with the brittle nature of HA, residual stress generated at the coating interface and the inconsistent formation of the oxide layer.

3.5. Failure modes of PEO coatings

In general, the failure modes mechanism observed in thin coatings is influenced by a number of internal and external factors. The internal factors are related to the testing conditions and are scratch test-dependent such as loading rate, indenter shape, scratch speed, machine calibration and others. The external factors are categorized as substrate material, coating properties, surface roughness, friction coefficient and testing environment [29]. Previous studies revealed the existence of a number of failure mode mechanisms, making the resulting behaviour of coatings subjected to the scratch test having a complex array of interaction of these factors [30].

In this study, the failure mechanism is divided into two stages. For the sample processed without HA addition, a chipping failure mode was observed, which implies that the TiO_2-PEO films on the Ti surface influence coating adhesion. The failure was seen to occur within the substrate, which leads to chipping and loss of coating along the scratch trackside (Fig. 5a). This may be due to the interaction of the coating and the substrate. The oxide film

Accepted manuscript

ACCEPTED MANUSCRIPT

is known to be brittle while Ti is ductile. As the diamond indenter contacts the coating during the scratch test, hemispherical chipping, which propagates outward from the centre line of the trackside, occurred due to compressive stresses generated ahead of the moving diamond indenter. Trackside chipping occurs due to compressive stresses that have been built up ahead of the moving diamond indenter. The stresses experienced by the coating are relieved through hemispherical chipping on both sides of the track.

For the sample produced with HA addition, the coating failure is characterized by partial and intermittent delamination (Figs. 5(b-d)). The stresses responsible for the coating delamination are a combination of the stresses remaining in the coating and the localized tensile stresses generated by the diamond indenter stylus. The failure mode occurred ahead of the moving indenter. The shear force scrapes the coating off the substrate. The tensile crack first forms at the weak coating/substrate interface ahead of the moving indenter due to compressive shear stress. This is usually accompanied by the rise and fall of diamond indenter penetration depth. The continued forward movement of the indenter tip increases the stress and leads to the growth of an interfacial tensile crack (Fig. 5c). Prior to failure mode, the space between the scratch widths becomes constant and the interfacial tensile crack decreases. At this particular point, the high compressive stress that had built up disappears and no delamination will be observed. Eventually, the spallation is then replaced by chipping and detachment of the coating along the trackside. The spalled regions are usually smaller with a lower number of cracks. As mentioned earlier, the adhesive strength of TiO_2/HA was 2099 mN. Conversely, a value 1247 mN was recorded with the microporous oxide film on Ti surface. These results show that by infiltrating Ca and P in the porous oxide film, the adhesive strength can be increased by about 68%.

4. Conclusions

Accepted manuscript

ACCEPTED MANUSCRIPT

The enrichment of the PEO-TiO_2 layer on Ti6Al4V surface with HA particles was successfully performed in a solitary Na_3PO_4 solution using PEO in a single step approach. The coating morphology, structure and adhesion were notably influenced by the HA concentration. The content of Ca and P incorporated into the oxide film increased with the HA concentration in the PEO-TiO_2 coatings; the coating thickness and surface roughness have a positive correlation with the HA level dispersed in the Na_3PO_4 solution. The thickness of the PEO-layer varied from 10-17 μm depending on the HA content. An inverse relationship was seen between the porosity and the HA concentration of the suspensions. With increasing HA concentration from 0 g/L to 2 g/L, the porosity level decreased dramatically. The surface composition of the Ca and P embedded in the PEO - oxide film was critically affected when treated with suspensions with an HA concentration above 1.5 g/L.

The adhesive strength of the enriched layer was significantly affected by the concentration of Ca and P in the film. As the HA concentration increased, more Ca and P infiltrated into the oxide film and eventually led to deterioration of the adhesive strength of the layer. However, by varying the concentration of HA, an adhesive strength up to 2099 mN for the film prepared with an HA concentration of 1.5 g/L was achieved, compared to 1247 mN for the film prepared with no HA.

A maximum scratch hardness of about 5 GPa was obtained for the coatings. The failure phenomenon for the sample processed with HA is different from that prepared without HA. The failure without HA addition was characterized with substantial periodic hemispherical chipping as the loading force increased, whereas intermittent delamination was observed for HA coated surfaces.

Accepted manuscript

Acknowledgements

ACCEPTED MANUSCRIPT

The authors would like to acknowledge the University of Malaya for providing the necessary resources and facilities for this study. This project was supported under the FRGS grant no. FP056-2015A and PPP grant No. PG186-2016A.

References

[1] F. Golestani-Fard, M.R. Bayati, H.R. Zargar, S. Abbasi, H.R. Rezaei, MAO-preparation of nanocrystalline hydroxyapatite-titania composite films: Formation stages and effect of the growth time, Mater. Res. Bull. 46 (2011) 2422–2426.

[2] L.P. Qiao, J. Lou, S.F. Zhang, B. Qu, W.H. Chang, R.F. Zhang, The entrance mechanism of calcium and phosphorus elements into micro arc oxidation coatings developed on Ti6Al4V alloy, Surf. Coat. Technol. 285 (2016) 187–196.

[3] S. Durdu, M. Usta, A.S. Berkem, Bioactive coatings on Ti6Al4V alloy formed by plasma electrolytic oxidation, Surf. Coat .Technol. 301 (2016) 85–93.

[4] U. Vijayalakshmi, K. Prabakaran, S. Rajeswari, Preparation and characterization of sol-gel hydroxyapatite and its electrochemical evaluation for biomedical applications, J Biomed Mater Res Part A. 87 (2008) 739–749.

[5] C.H. Quek, K.. A. Khor, P. Cheang, Influence of processing parameters in the plasma spraying of hydroxyapatite / Ti6Al4V composite coatings, J. Mater. Process. Technol. 90 (1999) 550–555.

[6] M. Farrokhi-Rad, T. Shahrabi, Effect of suspension medium on the electrophoretic deposition of hydroxyapatite nanoparticles and properties of obtained coatings, Ceram. Inter. 40 (2014) 3031–3039.

[7] A. Tahmasbi Rad, M. Solati-Hashjin, N.A.A. Osman, S. Faghihi, Improved bio-physical performance of hydroxyapatite coatings obtained by electrophoretic deposition at dynamic voltage, Ceram. Inter. 40 (2014) 12681–12691.

Accepted manuscript

ACCEPTED MANUSCRIPT

[8] S.A. Adeleke, A. Bushroa, M.K. Herliansyah, I. Sopyan, W.J. Basirun, M. Ladan, Preparation, scratch adhesion and anti-corrosion performance of TiO_2-MgO-BHA coating on Ti6Al4V implant by plasma electrolytic oxidation technique, J. Adhes. Sci. Technol. (2017) 1–12.

[9] S.A. Adeleke, I. Sopyan, A.R. Bushroa, Hydroxyapaptite layer formation on titanium alloys surface using micro-arc oxidation, J. Eng. Appl. Sci. 10 (2015) 10101–10108.

[10] M. Sandhyarani, N. Rameshbabu, K. Venkateswarlu, L. Rama Krishna, Fabrication, characterization and in-vitro evaluation of nanostructured zirconia/hydroxyapatite composite film on zirconium, Surf. Coat. Technol. 238 (2014) 58–67.

[11] D. Quintero, O. Galvis, J.A. Calderón, J.G. Castaño, F. Echeverría, Effect of electrochemical parameters on the formation of anodic films on commercially pure titanium by plasma electrolytic oxidation, Surf. Coat Technol. 258 (2014) 1223–1231.

[12] M.A. Faghihi-Sani, A. Arbabi, A. Mehdinezhad-Roshan, Crystallization of hydroxyapatite during hydrothermal treatment on amorphous calcium phosphate layer coated by PEO technique, Ceram. Inter. 39 (2013) 1793–1798.

[13] M. Sowa, M. Piotrowska, M. Widziołek, G. Dercz, G. Tylko, T. Gorewoda, A.M. Osyczka, W. Simka, Bioactivity of coatings formed on Ti-13Nb-13Zr alloy using plasma electrolytic oxidation, Mater. Sci. Eng. C. 49 (2015) 159–173.

[14] H.P. Teng, C.J. Yang, J.F. Lin, Y.H. Huang, F.H. Lu, A simple method to functionalize the surface of plasma electrolytic oxidation produced TiO_2 coatings for growing hydroxyapatite, Electrochim Acta. 193 (2016) 216–224.

[15] J.M. Albella, J.M. Montero, I., Martinez-Duart, A theory of avalanche breakdown during anodic oxidation, Electrochim Acta. 32 (1987) 255–258.

[16] Q. Ding, J., Liang, J., Hu, Li-t., Hao, J-c., Xue, Effects of sodium tungstate on characteristics of microarc oxidation coatings formed on magnesium alloy in silicate-

Accepted manuscript

ACCEPTED MANUSCRIPT

KOH electrolyte, Trans. Nonferrous Met. Soc. China. 17 (2007) 244–249.

[17] Z. Yao, L. Li, Z. Jiang, Adjustment of the ratio of Ca/P in the ceramic coating on Mg alloy by plasma electrolytic oxidation, Appl. Surf. Sci. 255 (2009) 6724–6728.

[18] F.C. Walsh, C.T.J. Low, R.J.K. Wood, K.T. Stevens, J. Archer, A.R. Poeton, A. Ryder, Plasma electrolytic oxidation (PEO) for production of anodised coatings on lightweight metal (Al, Mg, Ti) alloys, T I Met Finish. 87 (2009) 122–135.

[19] S. Durdu, Ö.F. Deniz, I. Kutbay, M. Usta, Characterization and formation of hydroxyapatite on Ti6Al4V coated by plasma electrolytic oxidation, J. Alloy. Compd. 551 (2013) 422–429.

[20] S. Abbasi, M.R. Bayati, F. Golestani-Fard, H.R. Rezaei, H.R. Zargar, F. Samanipour, V. Shoaei-Rad, Micro arc oxidized HAp-TiO_2 nanostructured hybrid layers-part I: Effect of voltage and growth time, Appl. Surf. Sci. 257 (2011) 5944–5949.

[21] Y. Bai, K.A. Kim, I.S. Park, S.J. Lee, T.S. Bae, M.H. Lee, In situ composite coating of titania-hydroxyapatite on titanium substrate by micro-arc oxidation coupled with electrophoretic deposition processing, Mater. Sci. Eng. B Solid-State Mater. Adv. Technol. 176 (2011) 1213–1221.

[22] W. Simka, A. Krząkała, D.M. Korotin, I.S. Zhidkov, E.Z. Kurmaev, S.O. Cholakh, K. Kuna, G. Dercz, J. Michalska, K. Suchanek, T. Gorewoda, Modification of a Ti-Mo alloy surface via plasma electrolytic oxidation in a solution containing calcium and phosphorus, Electrochim Acta. 96 (2013) 180–190.

[23] D.J. Blackwood, K.H.W. Seah, Influence of anodization on the adhesion of calcium phosphate coatings on titanium substrates, J. Biomed Mater Res Part A. 93 (2010) 1551–1556.

[24] S.J. Bull, E.G. Berasetegui, An overview of the potential of quantitative coating adhesion measurement by scratch testing, Tribol. Interface Eng. Ser. 51 (2006) 136–

Accepted manuscript

ACCEPTED MANUSCRIPT

165.

[25] A.R. Bushroa, H.H. Masjuki, M.R. Muhamad, B.D. Beake, Optimized scratch adhesion for TiSiN coatings deposited by a combination of DC and RF sputtering, Surf Coat Technol. 206 (2011) 1837–1844.

[26] D.J. Blackwood, K.H.W. Seah, Electrochemical cathodic deposition of hydroxyapatite: Improvements in adhesion and crystallinity, Mater. Sci. Eng. C. 29 (2009) 1233–1238.

[27] M. Sarraf, E. Zalnezhad, A.R. Bushroa, A.M.S. Hamouda, S. Baradaran, B. Nasiri-Tabrizi, A.R. Rafieerad, Structural and mechanical characterization of Al/Al_2O_3 nanotube thin film on TiV alloy, Appl. Surf. Sci. 321 (2014) 511–519.

[28] ASTM International, Standard Test Method for Scratch Hardness of Materials Using a Diamond Stylus, Designation, G171-03, in: 2009: pp. 1–7. http://www.astm.org.

[29] R.F. Bunshah, ed., Handbook of hard coatings:Deposition Technologies, Properties and Application, Noyes publications, New York, 2001.

[30] P. Nledengvist, S. Hogmark, Experiences from scratch testing of tribological PVD coatings, Tribol. Inter. 30 (1997) 507–516.

Accepted manuscript

Table 1. Process parameters for PEO coatings.

PEO parameters	Quantity
HA concentration (g/L)	0-2
Na_3PO_4 (M)	0.12
Voltage (V)	300
Current density (Adm^{-2})	0.5
Treatment time (min)	5

Table 2. Chemical composition of the PEO hydroxyapatite coatings.

	Sample code			
	S_0	S_1	$S_{1.5}$	S_2
Ca, at.%	-	13.43	17.57	22.84
P, at. %	9.86	11.93	14.52	17.58
Ca/P ratio	-	1.13	1.21	1.30

Table 3. Variation in surface roughness, porosity and thickness of PEO coatings as a function of HA concentration.

Sample code	HA (g/L)	R_a (μm)	Porosity (%)	Thickness (μm)
Ti	-	0.16	-	-
S_0	0	1.47	80.8	9.8
S_1	1.0	2.11	59.0	11.5
$S_{1.5}$	1.5	2.18	55.5	13.6
S_2	2.0	2.20	54.1	16.7

Accepted manuscript

ACCEPTED MANUSCRIPT

Fig. 1. Voltage-time plots obtained during the PEO process in different electrolyte concentration.

Fig. 2. Surface morphology of (a) Ti6Al4V and PEO ceramic coated samples for (b) S_0, (c) S_1, (d) $S_{1.5}$, and (e) S_2, with their corresponding EDX.

Fig. 3. XRD patterns of the PEO ceramic coatings obtained in NAP electrolyte solution with different HA concentrations (a) S_0, (b) S_1, (c) $S_{1.5}$, and (d) S_2

Fig. 4. FESEM cross-section images of the PEO coated samples for (a) S_0, (b) S_1, (c) $S_{1.5}$, and (d) S_2.

Fig. 5. Optical images of PEO hydroxyapatite coated surfaces during scratch test for (a) S_0, (b) S_1, (c) $S_{1.5}$, and (d) S_2, along with their corresponding load, depth and frictional force as a function of scratch length.

Fig. 6. FESEM images of the scratch test produced using the PEO process in the NAP electrolyte solution with HA concentration for (a) $S_{1.5}$ and (b) S_2, along with their corresponding line scan analysis.

Accepted manuscript

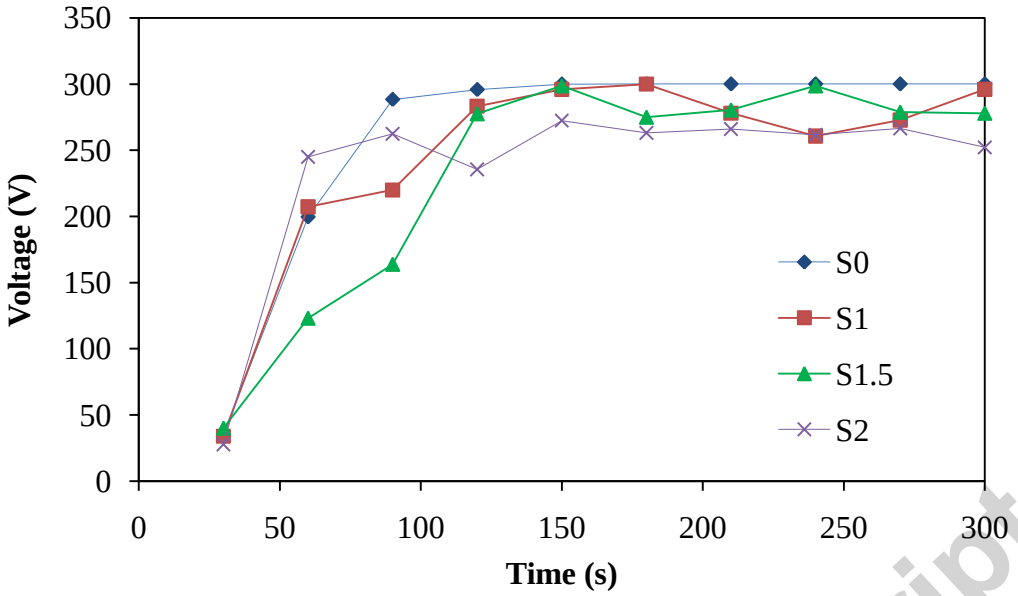

Accepted manuscript

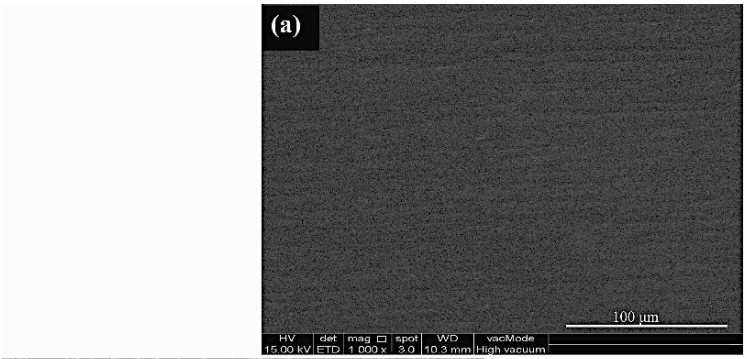

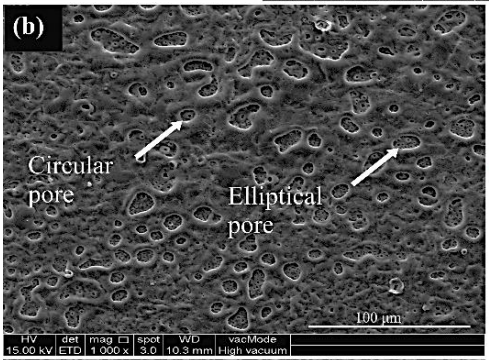

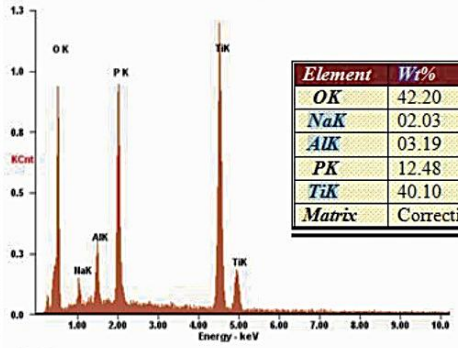

Element	Wt%	At%
OK	42.20	64.59
NaK	02.03	02.16
AlK	03.19	02.89
PK	12.48	09.86
TiK	40.10	20.50
Matrix	Correction	ZAF

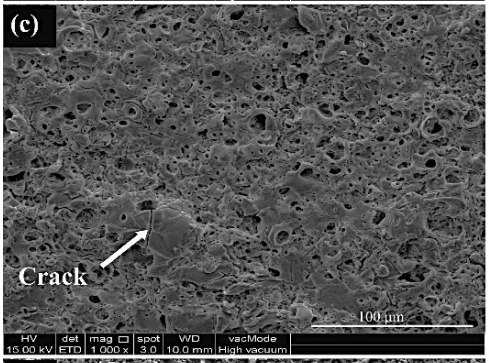

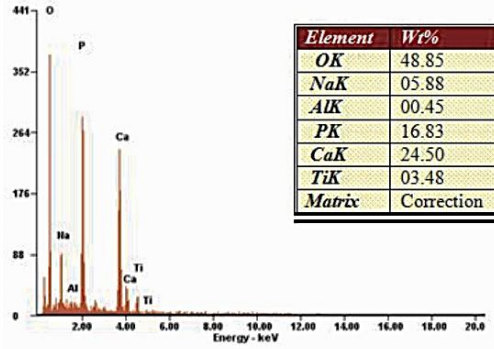

Element	Wt%	At%
OK	48.85	67.06
NaK	05.88	05.62
AlK	00.45	00.37
PK	16.83	11.93
CaK	24.50	13.43
TiK	03.48	01.60
Matrix	Correction	ZAF

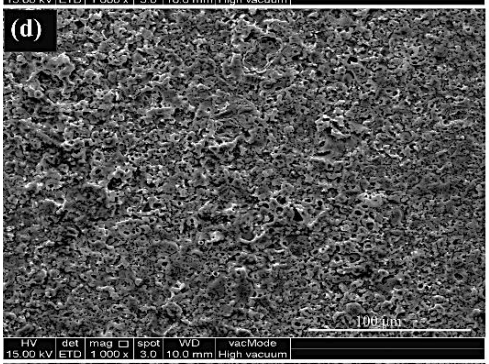

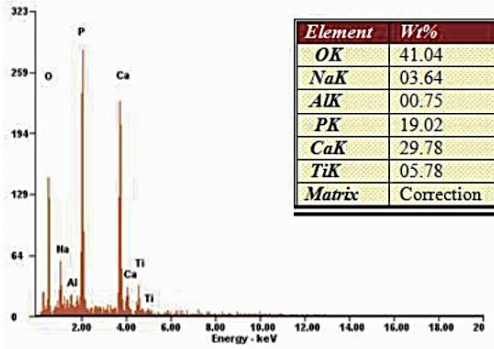

Element	Wt%	At%
OK	41.04	60.66
NaK	03.64	03.75
AlK	00.75	00.65
PK	19.02	14.52
CaK	29.78	17.57
TiK	05.78	02.85
Matrix	Correction	ZAF

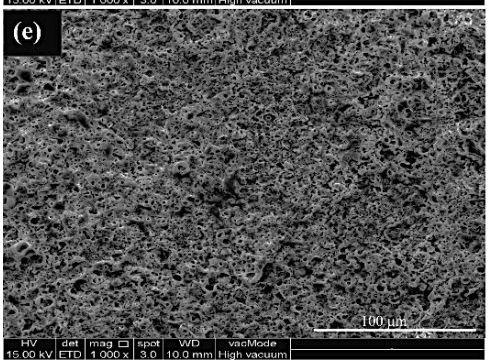

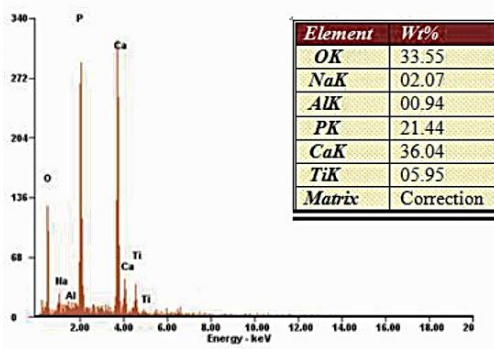

Element	Wt%	At%
OK	33.55	53.25
NaK	02.07	02.29
AlK	00.94	00.89
PK	21.44	17.58
CaK	36.04	22.84
TiK	05.95	03.16
Matrix	Correction	ZAF

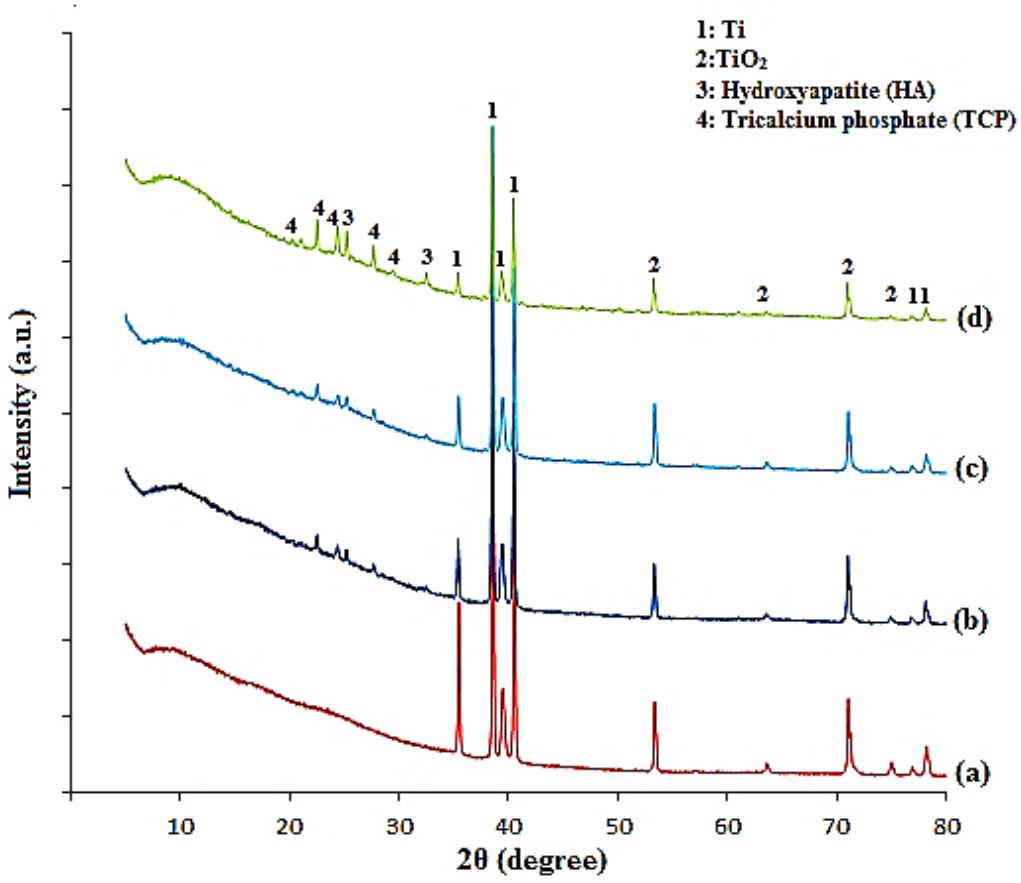
1: Ti
2:TiO2
3: Hydroxyapatite (HA)
4: Tricalcium phosphate (TCP)
Intensity (a.u.)
2θ (degree)
(a)
(b)
(c)
(d)

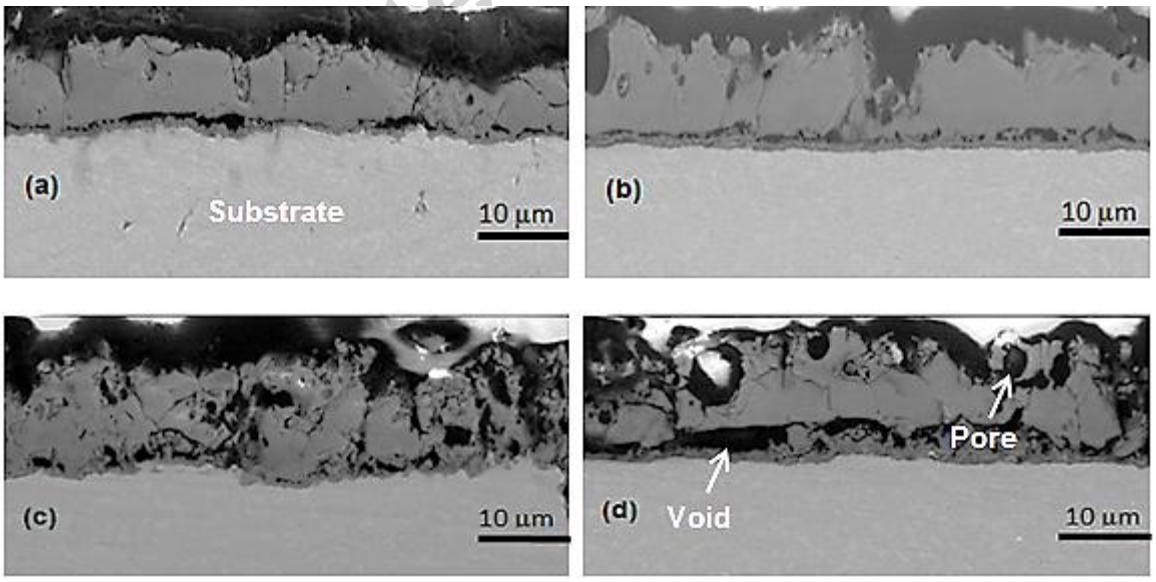
(a)
Substrate
10 µm
(b)
10 µm
(c)
10 µm
(d)
Void
Pore
10 µm

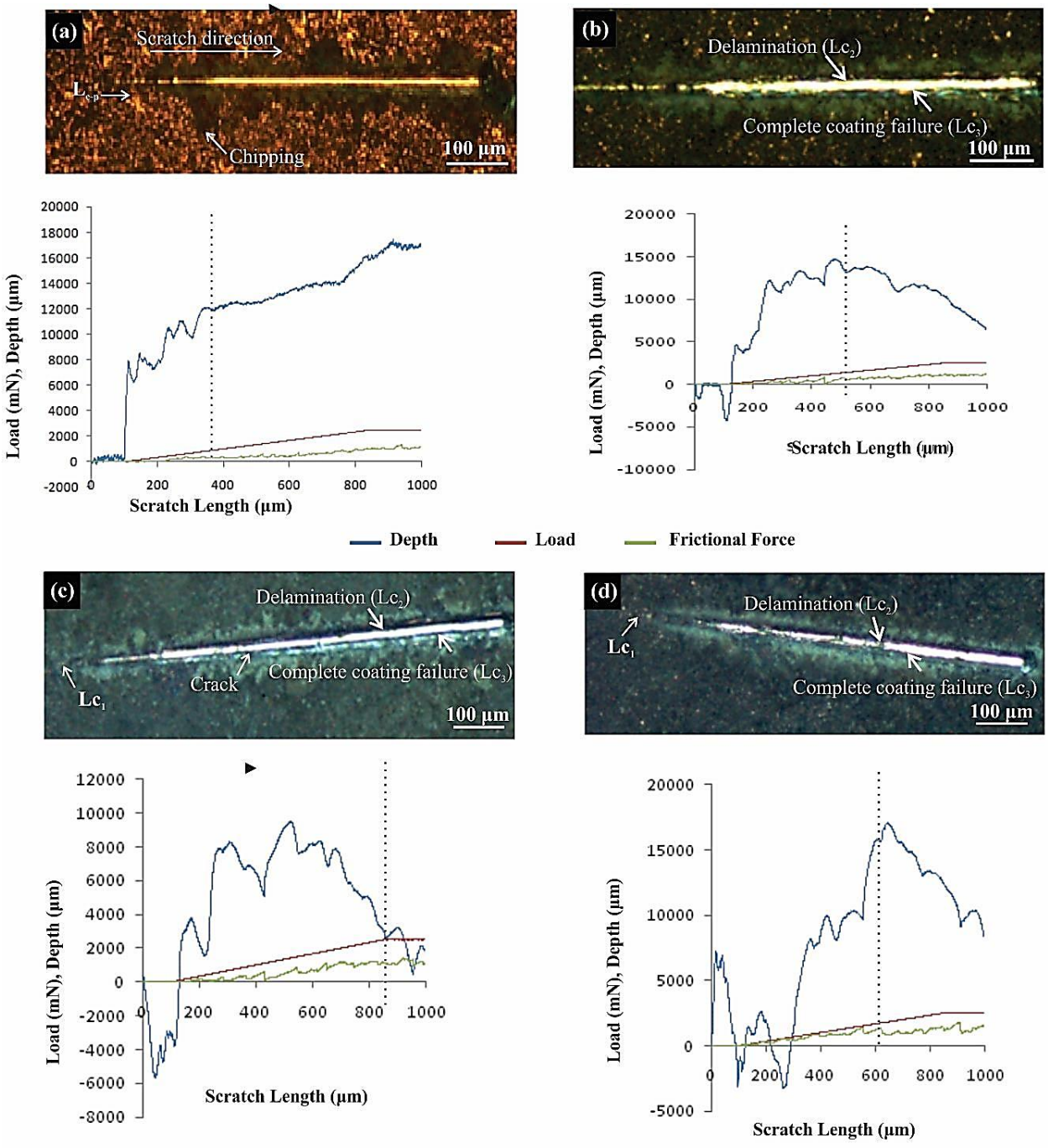
(a)
Scratch direction
L_{c_3}
Chipping
100 µm
(b)
Delamination (Lc_2)
Complete coating failure (Lc_3)
100 µm
Load (mN), Depth (µm)
Scratch Length (µm)
Depth
Load
Frictional Force
(c)
Delamination (Lc_2)
Crack
Complete coating failure (Lc_3)
Lc_1
100 µm
(d)
Delamination (Lc_2)
Lc_1
Complete coating failure (Lc_3)
100 µm

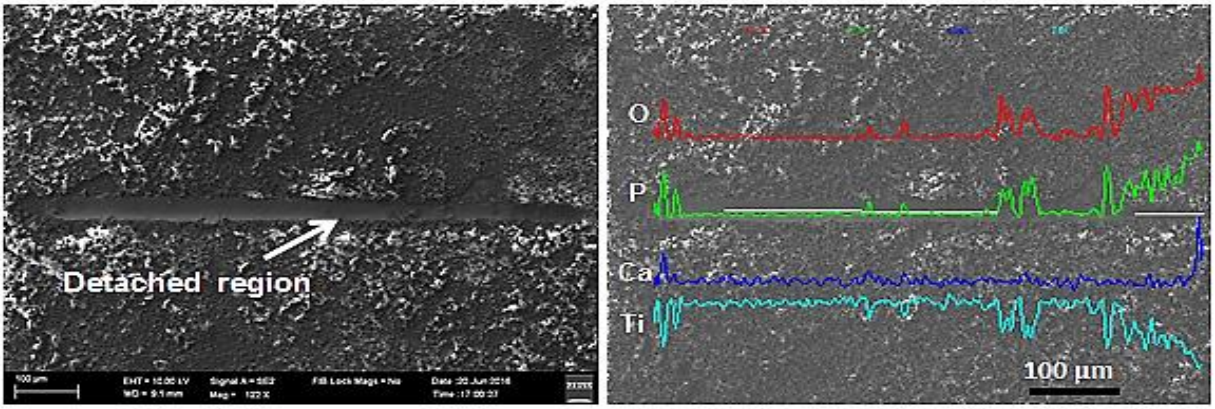

(a)

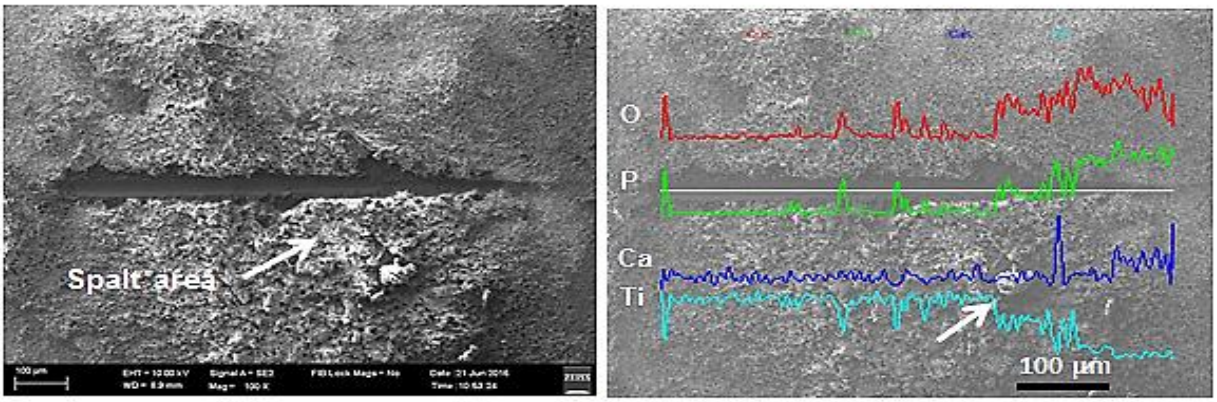

(b)

Accepted manuscript